

# High-intracavity-power thin-disk laser for the alignment of molecules

Bastian Deppe,<sup>1,2,3,4</sup> Günter Huber,<sup>1,2,3</sup> Christian Kränkel,<sup>1,2,3,5</sup>  
and Jochen Küpper<sup>1,2,4,6</sup>

<sup>1</sup>*The Hamburg Center for Ultrafast Imaging, University of Hamburg, Luruper Chaussee 149, 22761 Hamburg, Germany*

<sup>2</sup>*Department of Physics, University of Hamburg, Luruper Chaussee 149, 22761 Hamburg, Germany*

<sup>3</sup>*Institut für Laser-Physik, University of Hamburg, Luruper Chaussee 149, 22761 Hamburg, Germany*

<sup>4</sup>*Center for Free-Electron Laser Science, DESY, Notkestraße 85, 22607 Hamburg, Germany*

<sup>5</sup>*ckraenkel@physnet.uni-hamburg.de*

<sup>6</sup>*jochen.kuepper@cfel.de*

**Abstract:** We propose a novel approach for strong alignment of gas-phase molecules for experiments at arbitrary repetition rates. A high-intracavity-power continuous-wave laser will provide the necessary ac electric field of  $10^{10}$ – $10^{11}$  W/cm<sup>2</sup>. We demonstrate thin-disk lasers based on Yb:YAG and Yb:Lu<sub>2</sub>O<sub>3</sub> in a linear high-finesse resonator providing intracavity power levels in excess of 100 kW at pump power levels on the order of 50 W. The multi-longitudinal-mode operation of this laser avoids spatial-hole burning even in a linear standing-wave resonator. The system will be scaled up as in-vacuum system to allow for the generation of fields of  $10^{11}$  W/cm<sup>2</sup>. This system will be directly applicable for experiments at modern X-ray light sources, such as synchrotrons or free-electron lasers, which operate at various very high repetition rates. This would allow to record molecular movies through temporally resolved diffractive imaging of fixed-in-space molecules, as well as the spectroscopic investigation of combined X-ray–NIR strong-field effects of atomic and molecular systems.

© 2015 Optical Society of America

**OCIS codes:** (020.2649) Strong field laser physics; (020.6580) Stark effect; (020.7010) Laser trapping; (140.3580) Lasers, solid-state; (140.3615) Lasers, ytterbium; (140.4780) Optical resonators.

---

## References and links

1. We distinguish between alignment and orientation according to the usual convention, i. e., alignment refers to fixing one or more molecular axes in space, while orientation refers to the breaking of the “up-down” symmetry along one or more axes.
2. H. Stapelfeldt and T. Seideman, “Colloquium: Aligning molecules with strong laser pulses,” *Rev. Mod. Phys.* **75**, 543–557 (2003).
3. R. Neutze, R. Wouts, D. van der Spoel, E. Weckert, and J. Hajdu, “Potential for biomolecular imaging with femtosecond X-ray pulses,” *Nature* **406**, 752–757 (2000).
4. F. Filsinger, G. Meijer, H. Stapelfeldt, H. Chapman, and J. Küpper, “State- and conformer-selected beams of aligned and oriented molecules for ultrafast diffraction studies,” *Phys. Chem. Chem. Phys.* **13**, 2076–2087 (2011).
5. A. Barty, J. Küpper, and H. N. Chapman, “Molecular imaging using x-ray free-electron lasers,” *Annu. Rev. Phys. Chem.* **64**, 415–435 (2013).
6. J. Küpper, S. Stern, L. Holmegaard, F. Filsinger, A. Rouzée, A. Rudenko, P. Johnsson, A. V. Martin, M. Adolph, A. Aquila, S. Bajt, A. Barty, C. Bostedt, J. Bozek, C. Caleman, R. Coffee, N. Coppola, T. Delmas, S. Epp, B. Erk, L. Foucar, T. Gorkhover, L. Gumprecht, A. Hartmann, R. Hartmann, G. Hauser, P. Holl, A. Hömke,

- N. Kimmel, F. Krasniqi, K.-U. Kühnel, J. Maurer, M. Messerschmidt, R. Moshhammer, C. Reich, B. Rudek, R. Santra, I. Schlichting, C. Schmidt, S. Schorb, J. Schulz, H. Soltau, J. C. H. Spence, D. Starodub, L. Strüder, J. Thøgersen, M. J. J. Vrakking, G. Weidenspointner, T. A. White, C. Wunderer, G. Meijer, J. Ullrich, H. Stapelfeldt, D. Rolles, and H. N. Chapman, "X-ray diffraction from isolated and strongly aligned gas-phase molecules with a free-electron laser," *Phys. Rev. Lett.* **112**, 083002 (2014).
7. M. Altarelli, R. Brinkmann, M. Chergui, W. Decking, B. Dobson, S. Düsterer, G. Grübel, W. Graeff, H. Graafsma, J. Hajdu, J. Marangos, J. Pflüger, H. Redlin, D. Riley, I. Robinson, J. Rossbach, A. Schwarz, K. Tiedtke, T. Tschentscher, I. Vartaniants, H. Wabnitz, H. Weise, R. Wichmann, K. Witte, A. Wolf, M. Wulff, and M. Yurkov, "The technical design report of the European XFEL," Tech. rep., DESY, Hamburg, Germany (2007).
  8. Basic Energy Sciences Advisory Committee, "Report of the besac subcommittee on future x-ray light sources," (2013).
  9. H. Franz, O. Leupold, R. Röhlberger, S. V. Roth, O. H. Seeck, J. Spengler, J. Stempfer, M. Tischer, J. Viehhaus, E. Weckert, and T. Wroblewski, "Technical Report: PETRA III: DESY's new high brilliance third generation synchrotron radiation source," *Synchrotron Radiat. News* **19**, 25–29 (2006).
  10. A. Vaupel, N. Bodnar, B. Webb, L. Shah, and M. Richardson, "Concepts, performance review, and prospects of table-top, few-cycle optical parametric chirped-pulse amplification," *Opt. Eng.* **53**, (2014).
  11. B. Friedrich and D. Herschbach, "Alignment and trapping of molecules in intense laser fields," *Phys. Rev. Lett.* **74**, 4623–4626 (1995).
  12. L. Holmegaard, J. H. Nielsen, I. Nevo, H. Stapelfeldt, F. Filsinger, J. Küpper, and G. Meijer, "Laser-induced alignment and orientation of quantum-state-selected large molecules," *Phys. Rev. Lett.* **102**, 023001 (2009).
  13. S. Trippel, T. Mullins, N. L. M. Müller, J. S. Kienitz, K. Długołęcki, and J. Küpper, "Strongly aligned and oriented molecular samples at a kHz repetition rate," *Mol. Phys.* **111**, 1738 (2013).
  14. Y.-P. Chang, D. Horke, S. Trippel, and J. Küpper, "Spatially-controlled complex molecules and their applications," *Int. Rev. Phys. Chem.* **34**, 557–590 (2015). In press, DOI: 10.1080/0144235X.2015.1077838.
  15. S. Trippel, T. Mullins, N. L. M. Müller, J. S. Kienitz, J. J. Omiste, H. Stapelfeldt, R. González-Férez, and J. Küpper, "Strongly driven quantum pendulum of the carbonyl sulfide molecule," *Phys. Rev. A* **89**, 051401(R) (2014).
  16. J. H. Nielsen, H. Stapelfeldt, J. Küpper, B. Friedrich, J. J. Omiste, and R. González-Férez, "Making the best of mixed-field orientation of polar molecules: A recipe for achieving adiabatic dynamics in an electrostatic field combined with laser pulses," *Phys. Rev. Lett.* **108**, 193001 (2012).
  17. S. Trippel, T. Mullins, N. L. M. Müller, J. S. Kienitz, R. González-Férez, and J. Küpper, "Two-state wave packet for strong field-free molecular orientation," *Phys. Rev. Lett.* **114**, 103003 (2015).
  18. J. J. Larsen, K. Hald, N. Bjerre, H. Stapelfeldt, and T. Seideman, "Three dimensional alignment of molecules using elliptically polarized laser fields," *Phys. Rev. Lett.* **85**, 2470–2473 (2000).
  19. I. Nevo, L. Holmegaard, J. H. Nielsen, J. L. Hansen, H. Stapelfeldt, F. Filsinger, G. Meijer, and J. Küpper, "Laser-induced 3D alignment and orientation of quantum state-selected molecules," *Phys. Chem. Chem. Phys.* **11**, 9912–9918 (2009).
  20. T. Kierspel, J. Wiese, T. Mullins, J. Robinson, A. Aquila, A. Barty, R. Bean, R. Boll, S. Boutet, P. Bucksbaum, H. N. Chapman, L. Christensen, A. Fry, M. Hunter, J. E. Koglin, M. Liang, V. Mariani, A. Morgan, A. Natan, V. Petrovic, D. Rolles, A. Rudenko, K. Schnorr, H. Stapelfeldt, S. Stern, J. Thøgersen, C. H. Yoon, F. Wang, S. Trippel, and J. Küpper, "Strongly aligned molecules at free-electron lasers," *J. Phys. B* **48**, 204002 (2015).
  21. W. H. Benner, M. J. Bogan, U. Rohner, S. Boutet, B. Woods, and M. Frank, "Non-destructive characterization and alignment of aerodynamically focused particle beams using single particle charge detection," *J. Aerosol. Sci.* **39**, 917–928 (2008).
  22. R. A. Kirian, S. Awel, N. Eckerskorn, H. Fleckenstein, M. Wiedorn, L. Adriano, S. Bajt, M. Barthelmeß, R. Bean, K. R. Beyerlein, L. M. G. Chavas, M. Domaracky, M. Heymann, D. A. Horke, J. Knoska, M. Metz, A. Morgan, D. Oberthuer, N. Roth, T. Sato, P. L. Xavier, O. Yefanov, A. V. Rode, J. Küpper, and H. N. Chapman, "Simple convergent-nozzle aerosol injector for single-particle diffractive imaging with x-ray free-electron lasers," *Struct. Dyn.* **2**, 041717 (2015).
  23. N. R. Hutzler, H. I. Lu, and J. M. Doyle, "The buffer gas beam: An intense, cold, and slow source for atoms and molecules," *Chem. Rev.* **112**, 4803–4827 (2012).
  24. E. Shcherbakov, V. Fomin, A. Abramov, A. Ferin, D. Mochalov, and V. P. Gapontsev, "Industrial grade 100 kW power cw fiber laser," in "Advanced Solid-State Lasers Congress," (Optical Society of America, 2013), p. ATH4A.2.
  25. H. Aksakal and E. Arkan, "A feasibility study of tac ir-fel project," *Nucl. Instrum. Meth. A* **620**, 155 – 158 (2010).
  26. S. Mustafiz, N. Bjorndalen, and M. R. Islam, "Lasing into the future: Potentials of laser drilling in the petroleum industry," *Petrol. Sci. Technol.* **22**, 1187–1198 (2004).
  27. T. Y. Fan, "Laser beam combining for high-power, high-radiance sources," *IEEE J. Sel. Topics Quantum Electron.* **11**, 567–577 (2005).
  28. G. Mourou, B. Brocklesby, T. Tajima, and J. Limpert, "The future is fibre accelerators," *Nat. Photon.* **7**, 258–261 (2013).
  29. A. Giesen, H. Hügel, A. Voss, K. Wittig, U. Brauch, and H. OPOWER, "Scalable concept for diode-pumped high-power solid-state lasers," *Appl. Phys. B* **58**, 365–372 (1994).

30. A. Giesen, "Scaling thin disk lasers to high power and energy," in "CLEO: 2013," (Optical Society of America, 2013), p. CTu10.1.
31. T. Gottwald, V. Kuhn, S.-S. Schad, C. Stolzenburg, and A. Killi, "Recent developments in high power thin disk lasers at TRUMPF Laser," Proc. SPIE **8898**, 88980p (2013).
32. S. Stern, L. Holmegaard, F. Filsinger, A. Rouzee, A. Rudenko, P. Johnsson, A. V. Martin, A. Barty, C. Bostedt, J. Bozek, R. Coffee, S. Epp, B. Erk, L. Foucar, R. Hartmann, N. Kimmel, K.-U. Kühnel, J. Maurer, M. Messerschmidt, B. Rudek, D. Starodub, J. Thøgersen, G. Weidenspointner, T. A. White, H. Stapelfeldt, D. Rolles, H. N. Chapman, and J. Küpper, "Toward atomic resolution diffractive imaging of isolated molecules with x-ray free-electron lasers," Faraday Disc. **171**, 393 (2014).
33. A. T. J. B. Eppink and D. H. Parker, "Velocity map imaging of ions and electrons using electrostatic lenses: Application in photoelectron and photofragment ion imaging of molecular oxygen," Rev. Sci. Instrum. **68**, 3477–3484 (1997).
34. R. Peters, C. Kränkel, K. Petermann, and G. Huber, "Crystal growth by the heat exchanger method, spectroscopic characterization and laser operation of high-purity Yb:Lu<sub>2</sub>O<sub>3</sub>," J. Cryst. Growth **310**, 1934–1938 (2008).
35. L. Gmelin, *Gmelin Handbuch der anorganischen Chemie: Seltenerdelemente* (Springer-Verlag, 1974), vol. C1.
36. R. Peters, C. Kränkel, K. Petermann, and G. Huber, "Broadly tunable high-power Yb:Lu<sub>2</sub>O<sub>3</sub> thin disk laser with 80 % slope efficiency," Opt. Exp. **15**, 7075–7082 (2007).
37. C. Kränkel, "Rare-earth-doped sesquioxides for diode-pumped high-power lasers in the 1-, 2-, and 3- $\mu$ m spectral range," IEEE J. Sel. Topics Quantum Electron. **21**, 250–262 (2014).
38. J. A. Caird, S. A. Payne, P. R. Staver, A. J. Ramponi, L. L. Chase, and W. F. Krupke, "Quantum electronic properties of the Na<sub>3</sub>Ga<sub>2</sub>Li<sub>3</sub>F<sub>12</sub>:Cr<sup>3+</sup> laser," IEEE J. Quant. Elec. **24**, 1077–1099 (1988).
39. U. Wolters, "Inversion Dependent Losses in Yb: YAG and Their Effects on Thin-Disk Laser Operation," Ph.D. thesis, Universität Hamburg, Hamburg, Germany (2014).
40. C. Kränkel, C. J. Saraceno, O. H. Heckl, C. R. E. Baer, M. Golling, Südmeyer, K. Beil, Petermann, G. Huber, and U. Keller, "Ultrafast and high power thin disk lasers," in "2nd EOS Topical Meeting on Lasers (ETML'11)," (2011).
41. S. T. Fredrich-Thornton, "Nonlinear losses in single crystalline and ceramic Yb:YAG thin-disk lasers," Ph.D. thesis, Universität Hamburg (2010).
42. M. Larionov, "Kontaktierung und Charakterisierung von Kristallen für Scheibenlaser," Ph.D. thesis, Universität Stuttgart (2009).
43. H. Carstens, N. Lilienfein, S. Holzberger, C. Jocher, T. Eidam, J. Limpert, A. Tünnermann, J. Weitenberg, D. C. Yost, A. Alghamdi, Z. Alahmed, A. Azzeer, A. Apolonski, E. Fill, F. Krausz, and I. Pupeza, "Megawatt-scale average-power ultrashort pulses in an enhancement cavity," Opt. Lett. **39**, 2595 (2014).
44. J. Zhang, J. Brons, N. Lilienfein, E. Fedulova, V. Pervak, D. Bauer, D. Sutter, Z. Wei, A. Apolonski, O. Pronin, and F. Krausz, "260-megahertz, megawatt-level thin-disk oscillator," Opt. Lett. **40**, 1627–4 (2015).
45. V. Magni, "Multielement stable resonators containing a variable lens," J. Opt. Soc. Am. A **4**, 1962–1969 (1987).
46. K. Beil, S. T. Fredrich-Thornton, F. Tellkamp, R. Peters, C. Kränkel, K. Petermann, and G. Huber, "Thermal and laser properties of Yb:LuAG for kW thin disk lasers," Opt. Exp. **18**, 20712–20722 (2010).
47. C. R. E. Baer, O. H. Heckl, C. J. Saraceno, C. Schriber, C. Kränkel, T. Südmeyer, and U. Keller, "Frontiers in passively mode-locked high-power thin disk laser oscillators," Opt. Exp. **20**, 7054–7065 (2012).
48. C. J. Saraceno, F. Emaury, O. H. Heckl, C. R. E. Baer, M. Hoffmann, C. Schriber, M. Golling, T. Südmeyer, and U. Keller, "275 W of output power from a femtosecond thin disk oscillator operated in a vacuum environment," Opt. Exp. **20**, 23535–23541 (2012).
49. B. Weichelt, D. Blazquez-Sanchez, A. Austerschulte, A. Voss, T. Graf, and A. Killi, "Improving the brightness of a multi-kw thin disk laser with a single disk by an aspherical phase-front correction," Proc. SPIE **7721**, 77210M–77210M–8 (2010).
50. G. Scoles, *Atomic and Molecular Beam Methods* (Oxford University Press, 1988), vol. 1.
51. R. Boll, D. Anielski, C. Bostedt, J. D. Bozek, L. Christensen, R. Coffee, S. De, P. Declava, S. W. Epp, B. Erk, L. Foucar, F. Krasnqi, J. Küpper, A. Rouzee, B. Rudek, A. Rudenko, S. Schorb, H. Stapelfeldt, M. Stener, S. Stern, S. Techert, S. Trippel, M. J. J. Vrakking, J. Ullrich, and D. Rolles, "Femtosecond photoelectron diffraction on laser-aligned molecules: Towards time-resolved imaging of molecular structure," Phys. Rev. A **88**, 061402(R) (2013).
52. H. J. Loesch, "Orientation and alignment in reactive beam collisions – recent progress," Annu. Rev. Phys. Chem. **46**, 555–594 (1995).
53. R. Grimm, M. Weidemüller, and Y. B. Ovchinnikov, "Optical dipole traps for neutral atoms," in "Adv. At. Mol. Opt. Phys.," **42**, pp. 95–170 (2000).
54. A. Ashkin, "Acceleration and trapping of particles by radiation pressure," Phys. Rev. Lett. **24**, 156–159 (1970).
55. N. Eckerskorn, L. Li, R. A. Kirian, J. Küpper, D. P. DePonte, W. Krolikowski, W. M. Lee, H. N. Chapman, and A. V. Rode, "Hollow Bessel-like beam as an optical guide for a stream of microscopic particles," Opt. Exp. **21**, 30492–30499 (2013).
56. T. Mazza, M. Ilchen, A. J. Rafipoor, C. Callegari, P. Finetti, O. Plekan, K. C. Prince, R. Richter, M. B. Danailov, A. Demidovich, G. De Ninno, C. Grazioli, R. Ivanov, N. Mahne, L. Raimondi, C. Svetina, L. Avaldi, P. Bolognesi,

## 1. Introduction

Many experiments aiming at recording so-called “molecular movies” – the atomic-resolution imaging of the intrinsic structural dynamics of molecules – rely on molecules fixed-in-space, i. e., aligned or oriented samples of molecules [1, 2]. One of the most promising approaches is coherent X-ray diffractive imaging, for instance, using short-wavelength free-electron lasers or synchrotrons [3–6]. These modern light sources, especially upcoming free-electron lasers with very large photon fluxes such as the European XFEL [7] or LCLS II [8], but also synchrotrons [9] as well as table-top laser systems based on optical-parametric chirped-pulse amplification (OPCPA) [10], operate at very high repetition rates with ten-thousands to millions of pulses per second, sometimes in burst modes, which have to be matched by the high-intensity optical control lasers.

The alignment of gas-phase ensembles of molecules exploits the interaction between the anisotropic polarizability of the molecule and non-resonant linearly or elliptically, polarized electric fields [2, 11]. The electric field strengths necessary for strong (quasi) adiabatic alignment are on the order of  $10^{10}$ – $10^{12}$  W/cm<sup>2</sup>, even when exploiting very cold samples [12–14], and must be applied over durations longer than, or at least comparable to, the rotation periods of the molecules [15]. These range from tens of picoseconds for small molecules to nanoseconds or even microseconds for larger molecules. Adiabatic mixed-field orientation requires the addition of a moderate dc electric field and even longer laser pulses [12, 16, 17]. Three-dimensional control requires elliptically polarized fields with fully controllable ellipticity [18, 19]. Traditionally, injection-seeded Nd:YAG lasers operating at a repetition rate of some 10 Hz were used to provide the necessary fields. Recently, we have demonstrated the use of chirped pulses from amplified Ti:Sapphire laser systems at 1 kHz [13, 15] and the implementation of this amplified-chirped-pulse technique at the Linac Coherent Light Source (LCLS) at 120 Hz [20]. Continuous-wave (CW) lasers would allow for the control of molecules at arbitrary repetition rates. Furthermore, they would enable long interaction times. For instance, molecules or particles traveling through a 50  $\mu$ m laser beam with a velocity of 100 m/s [21–23] would experience an effective pulse duration of 0.5  $\mu$ s. However, the use of CW lasers to provide the envisioned field strengths with focal beam waists in excess of  $\omega_0 = 10$   $\mu$ m would require optical power levels of 30–300 kW, respectively, with a beam quality that allows for such tight focusing with a Rayleigh length comparable to the molecular beam diameter on the order of 1 mm.

100-kW-class CW lasers have been realized as fiber lasers [24], as CO<sub>2</sub> lasers [25] and as chemical deuterium fluoride lasers [26]. Coherent beam combining [27] is also a viable approach to achieve laser output at this power level [28]. The thin-disk laser (TDL) geometry has been shown to be suited for very high CW output powers in combination with Yb<sup>3+</sup>-doped gain materials [29]. Outputs exceeding 27 kW were demonstrated [30] and 100-kW-systems are anticipated [30, 31]. However, so far these high output powers of thin-disk lasers and fiber lasers are only available at beam qualities [24, 31] that do not allow for the tight focusing necessary to achieve the envisioned focal intensities. In contrast, carbon dioxide and chemical lasers have good beam qualities at even higher output power, but their demanding space requirements and the possibly toxic gain materials are a significant drawback for using the setup as a mobile user facility at modern X-ray light sources. Moreover, operating and propagating any laser at such high output power levels imposes serious safety risks.

Here, we propose to provide the necessary field strength in an intracavity focus of a CW TDL

resonator. A resonator with low losses, low output coupler transmission, and high intracavity power has a low stored excitation energy in the crystal, a high photon energy storage in the resonator and comparably low output power. The required pump power levels are reasonably low due to the strong enhancement in the active cavity and allow for a cost efficient system, without an exceptional laser-safety risk. In combination with its small spatial footprint, such a system is an ideal candidate for flexible and safe employment at modern light sources. A long multiply-folded resonator allows for TEM<sub>00</sub> operation and enables to focus the beam with the necessary Rayleigh length of 1-mm.

## 2. Design criteria for an high-intracavity-power Yb<sup>3+</sup>-based continuous-wave laser

The envisioned aligned-molecule-imaging experiments impose a number of design criteria on the TDL. These arise partly from the actual molecular physics and partly from the need for integration of the alignment laser into the complex and constraining machinery of the experimental setup, schematically shown in Fig. 1. The ultra-high-vacuum needs impose further restrictions on the design of the setup.

In order to ensure the alignment of all probed molecules, the electric field intensity of  $\sim 10^{11}$  W/cm<sup>2</sup> utilized to control the molecules, has to be spatially and temporally smooth and nearly constant over the diffraction volume. The latter is defined by the overlap of the few-mm-diameter molecular beam and the 10- $\mu$ m-diameter X-ray-beam. Such a homogeneous field can be achieved inside the TDL resonator through multi-longitudinal-mode operation, as depicted in the inset of Fig. 1. The different modes average out the field distribution around the interaction point. For a few ten modes a longitudinally practically homogeneous field is achieved in the resonator. Under these conditions, spatial hole burning could only occur close to the end mirrors. Multi-longitudinal mode operation does not impose a serious challenge for the bandwidth of the laser material or the resonator design. At a typical lengths of a TEM<sub>00</sub> TDL of 1 m, hundreds of longitudinal modes fit into 1 pm of laser emission bandwidth in the 1  $\mu$ m wavelength range. Yb<sup>3+</sup>-doped lasers typically exhibit emission bands with much broader bandwidths in the nanometer range.

The laser beam needs to be focused to create the necessary field strength. At the same time, the TDL beam needs to be larger than the X-ray beams, which are typically kept on the order of 10  $\mu$ m to avoid radiation damage [6, 32], and its Rayleigh length needs to be long enough to

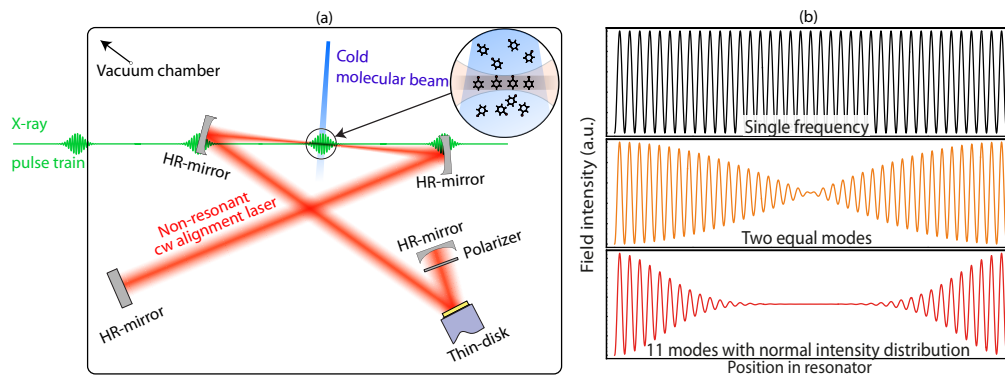


Fig. 1. (a): Concept for CW alignment of molecules: a high-finesse resonator in linearly polarized TEM<sub>00</sub> operation, focused inside of a vacuum chamber leads to the required focal intensities for alignment of molecules. (b): Mode averaging in the resonator yields in smooth intensity distribution and avoids spatial hole burning.

provide the necessary field strength over the width of the molecular beam of typically a few mm. This results in an envisioned focal waist of the TDL of approximately 20–40  $\mu\text{m}$ . Such small focal spot sizes require sophisticated astigmatism compensation, which has to be considered in the resonator design. Furthermore, a stable linear or elliptical polarization state is required.

The cold molecular beam has to be delivered to the intracavity focus and the degree of alignment needs to be monitored, for instance, through velocity map ion imaging (VMI) [33]. At the current state, the dimensions of the delivery mechanics and the VMI device require a clear space of tens of  $\text{cm}^3$  around the focus. Moreover, the X-ray beam must pass the focus nearly collinear with the TDL intracavity mode to achieve a good overlap with the volume of strongly aligned molecules.

Finally, the laser wavelength must be off-resonant with respect to the molecular sample to avoid excitation and radiation damage from the control beam. As the electronic transitions of molecules are typically in the ultraviolet or visible spectral range and vibrational excitations in the mid-infrared range, this requirement is usually fulfilled by  $\text{Yb}^{3+}$ -based lasers with emission wavelengths around 1  $\mu\text{m}$ .

### 3. Experimental setup

In a first proof-of-principle experiment a TDL was set up in a short longitudinal resonator. This allowed to characterize different gain materials at low output coupler transmissions with respect to their losses and their efficiencies. The experiments were carried out utilizing a  $\text{Yb}(7\%):\text{Y}_3\text{Al}_5\text{O}_{12}$  (Yb:YAG) disk (Dausinger+Giesen) with a thickness of 0.22 mm and a  $\text{Yb}(3\%):\text{Lu}_2\text{O}_3$  disk with a thickness of 0.25 mm [34]. Due to the different cation densities [35] in both host materials, the different values for the  $\text{Yb}^{3+}$ -doping correspond to a similar  $\text{Yb}^{3+}$ -density of  $\sim 10^{21} \text{ cm}^{-3}$ . Both disks were soldered onto copper-tungsten-alloy heat-sinks (20/80 for Yb:YAG and 10/90 for Yb: $\text{Lu}_2\text{O}_3$ ), which were cooled at a water temperature of 6  $^\circ\text{C}$  during the experiments. The disks were pumped by 600  $\mu\text{m}$ -core multimode fiber coupled InGaAs laser diodes, which were imaged onto a 1.2 mm diameter pump spot on the disk. For the Yb:YAG disk a pump wavelength of 940 nm corresponding to a broad Yb:YAG absorption band in this wavelength range was chosen. The Jenoptik JOLD-75-CPXF-2P laser diode utilized for this purpose had a maximum output power of 75 W and up to 56 W were used in the experiments. In contrast, Yb: $\text{Lu}_2\text{O}_3$  provides a much stronger absorption at the zero-phonon line around 976 nm [36]. The corresponding JOLD-50-CPXF-2P pump laser diode provided up to 50 W of output power which was fully utilized. The temperature of the pump diodes was adjusted to fine-tune the emission wavelength for an optimum absorption of the pump power. After the 24 pump-light passes in our TDL module, more than 99 % of the pump power was absorbed. A simple plane-concave resonator with a length of 60 mm and different output coupling mirrors with radii of curvature (ROC) of 100 mm (ROC of the disks  $\approx 2$  m) was set up for efficient multimode laser operation. The output-coupling mirrors had transmissions between  $9.5 \times 10^{-5}$  and  $4 \times 10^{-3}$  for all wavelengths between 1  $\mu\text{m}$  and 1.1  $\mu\text{m}$ . The output coupler transmissions were initially measured with a spectrometer (Varian Cary 5000) and cross-checked by measuring the transmission of the output of a Yb: $\text{Lu}_2\text{O}_3$  TDL operating at wavelength of 1080 nm through these mirrors. The laser output power was measured with a Coherent LM-100 power meter. To avoid damage of the disks we limited the maximum pump power to the value which resulted in a disk surface temperature of  $\approx 120$   $^\circ\text{C}$ . For this purpose we monitored the surface temperature of the laser disks with a SC645 thermographic camera (FLIR Systems). The measured values were corrected by the temperature dependent emissivity of the respective gain material. The emission spectra of the lasers were measured with a spectrometer (Ocean Optics HR2000), suitable for the wavelength range between 950 nm and 1100 nm.

#### 4. Experimental results

In Fig. 2 (a) the laser performance of the Yb:YAG and the Yb:Lu<sub>2</sub>O<sub>3</sub> disks are shown for three output coupler transmissions of  $9.5 \times 10^{-5}$ ,  $5 \times 10^{-4}$ ,  $4 \times 10^{-3}$ . The observed slope efficiencies as well as the measured surface temperatures for these and other mirrors for a pump power of 50 W are shown in Fig. 2 (b). As the surface temperature of Yb:Lu<sub>2</sub>O<sub>3</sub> exceeded a damage-critical temperature of 130°C for the lowest output coupler transmission, the maximum pump power was limited to 47 W for this mirror. For Yb:YAG and Yb:Lu<sub>2</sub>O<sub>3</sub> maximum slope efficiencies of 67 % and 72 % were measured at the highest output coupler transmission rate of  $4 \times 10^{-3}$  with a maximum output power of 36 W and 34 W, respectively. In this configuration, the maximum optical-to-optical efficiency was 66 % and 68 %, respectively. It should be noted that these  $T_{oc}$  are significantly below the optimum  $T_{oc}$  for maximum laser output for these materials [36]. Thus, the efficiencies reported here are lower than previously reported [37]. However, from the measured efficiencies it can be concluded that the losses through the output coupling mirror are significantly higher than the losses in the disks at these output coupler transmissions. For both materials, this results in low surface temperatures even at pump powers of 50 W, which range from around 50°C for large output coupler transmissions to the highest surface temperatures of 85°C and 127°C for Yb:YAG and Yb:Lu<sub>2</sub>O<sub>3</sub>, respectively, measured at the lowest output coupler transmission rate of  $9.5 \times 10^{-5}$ . Here, the losses in the disks mainly cause a strong heating of the laser disks as they dominate over the output coupler transmission losses. Despite this relatively strong heating, for both lasers no thermal roll over could be observed, and maximum output powers  $P_{out}$  of 13 W and 10 W were reached, respectively. From these numbers the intracavity power  $P_{int}$  was derived from the known output coupler transmission  $T_{out}$  as

$$P_{int} = \frac{P_{out}}{T_{oc}}. \quad (1)$$

Both disks achieved their highest CW intracavity power of 137 kW for Yb:YAG and 105 kW for Yb:Lu<sub>2</sub>O<sub>3</sub> at minimized total resonator losses, i. e., at the lowest output coupler transmission rate of  $9.5 \times 10^{-5}$ . At such low output coupler transmissions the laser spectrum of Yb:YAG covers wavelengths between 1050 nm and 1085 nm, while the Yb:Lu<sub>2</sub>O<sub>3</sub> laser oscillates at wavelengths between 1078 nm and 1082 nm. From the laser performance at different/lowest output coupler transmissions, we derived the resonator round-trip losses by the Caird analysis [38]. The slope

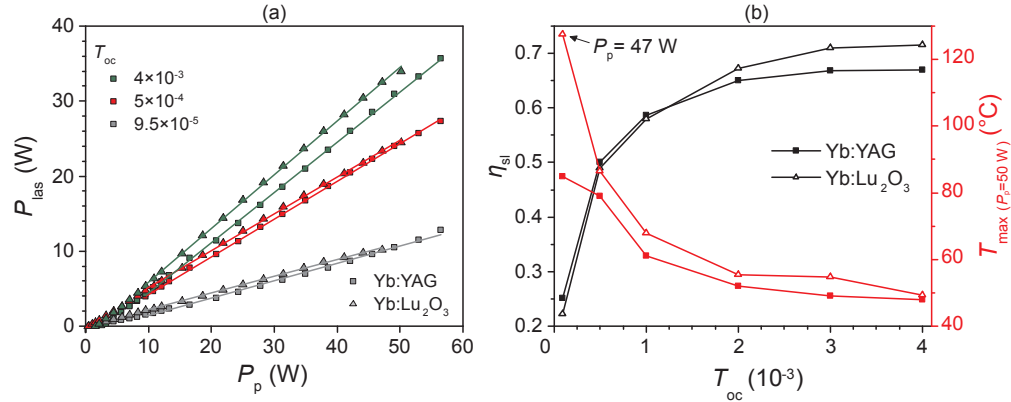


Fig. 2. (a) Laser performance of a 0.22 mm thick Yb:YAG disk and a 0.25 mm thick Yb:Lu<sub>2</sub>O<sub>3</sub> disk for different output coupler transmissions. (b) Slope efficiency and surface temperature ( $P_p = 50$  W) for different output coupler transmissions.

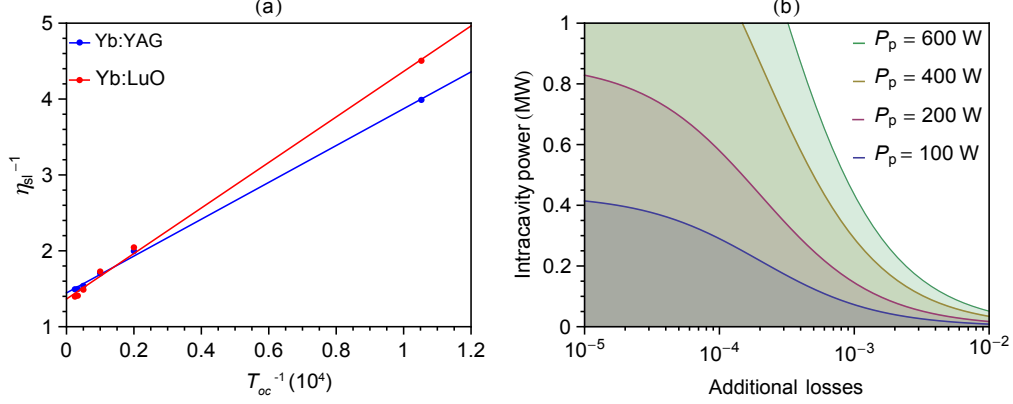


Fig. 3. (a) Caird analysis of the Yb:YAG and Yb:Lu<sub>2</sub>O<sub>3</sub> disk according to Eq. 3. (b) Calculated intracavity power for internal losses of  $2 \times 10^{-4}$  for fixed pump powers against additional losses.

efficiency  $\eta_{sl}$  of a laser follows from

$$\eta_{sl} = \eta_{oc} \cdot \eta_{St} \cdot \eta_{abs} \cdot \eta_{ov}. \quad (2)$$

with the the output coupling efficiency  $\eta_{oc} = T_{oc}/(T_{oc} + L_{int})$ , the Stokes efficiency  $\eta_{St}$ , the pump absorption efficiency  $\eta_{abs}$ , and the pump-laser mode overlap efficiency  $\eta_{ov}$ . The product of the latter three can be abbreviated as total efficiency  $\eta_{tot} = \eta_{St} \cdot \eta_{abs} \cdot \eta_{ov}$ . Trivial rearrangements lead to

$$\frac{1}{\eta_{sl}} = \frac{L_{int}}{\eta_{tot}} \cdot \frac{1}{T_{oc}} + \frac{1}{\eta_{tot}} \quad (3)$$

which allows to derive the resonator losses from a linear fit of the inverted slope efficiencies versus the inverted output coupler transmission. It is known that the Caird plot may not lead to reasonable results at higher output coupler transmissions, where the slope efficiency decreases due to loss processes at high inversion densities which are not covered by the underlying rate equations [39]. However, at the low output coupler transmissions used in our experiments, these effects are negligible. The fit according to Eq. 3 is shown in Fig. 3 (a) and results in very low round-trip losses of  $1.7 \times 10^{-4}$  for Yb:YAG and only slightly higher losses of  $2.2 \times 10^{-4}$  for Yb:Lu<sub>2</sub>O<sub>3</sub>. The total efficiency amounts to 71 % for Yb:YAG and 77 % for Yb:Lu<sub>2</sub>O<sub>3</sub>.

Considering the slope efficiencies  $\eta_{sl}$  approaching the Stokes efficiencies  $\eta_{st} = \lambda_{las}/\lambda_p$  previously observed in TDLs [40] one might argue that the absorption efficiency  $\eta_{abs}$  and the overlap efficiency of pump and laser mode  $\eta_{ov}$  should be approaching unity. This condition is fulfilled by deriving the intracavity losses from the ratio of the Stokes efficiency  $\eta_{st}$  and the slope efficiency  $\eta_{sl}$  at the lowest output coupler transmission from

$$L_{int,max} = \left( \frac{\eta_{St}}{\eta_{sl}} - 1 \right) T_{oc} \quad (4)$$

Despite the higher Stokes efficiency of  $\eta_{St} \approx 0.9 > \eta_{tot}$ , even in this case the corresponding losses are only slightly higher and amount to  $2.4 \times 10^{-4}$  for Yb:YAG and  $2.9 \times 10^{-4}$  for Yb:Lu<sub>2</sub>O<sub>3</sub>. Nota bene, this is an upper level for the intracavity losses due to energy conservation.

The intracavity power considering realistic resonator losses of  $L_{int} = 2 \times 10^{-4}$  plus additional losses  $L_{add}$  between  $10^{-5}$  and  $10^{-2}$  due to output coupler transmission or other intracavity elements required e.g. for the polarization selection were calculated for pump powers  $P_p$  between

100 W and 600 W with

$$P_{\text{int}} = \left( \frac{1}{L_{\text{add}} + L_{\text{int}}} \right) \cdot \eta_{\text{st}} \cdot (P_{\text{p}} - P_{\text{thr}}). \quad (5)$$

This equation can be simplified by assuming a threshold power  $P_{\text{thr}}$  of zero, which is appropriate as pump thresholds  $< 0.5$  W were observed in all experiments. The resulting intracavity powers are depicted in Fig. 3 (b).

## 5. Discussion

All measurements were performed in a short linear laser resonator to allow for both, efficient multi-mode lasing and for easy evaluation of losses, which require knowledge of the specific loss of all optical components. Under these conditions the gain-medium-specific resonator losses  $L_{\text{int}} \leq 2 \times 10^{-4}$  can be nearly exclusively attributed to losses in the TDL assembly, i. e., the laser-medium disk with its dielectric coatings and the metallic contacting layer. While the Yb:YAG disk showed in general better performance, our experiments do not provide conclusive evidence about the material-specific advantage of Yb:YAG or Yb:Lu<sub>2</sub>O<sub>3</sub>. Using a pump power of 54 W we achieved an intracavity power of 135 kW for Yb:YAG. This is to the best of our knowledge the highest documented CW intracavity power for a pump power lower than 100 W. Typically, such CW intracavity powers are only achieved using pump powers of 10 kW.

The slope efficiencies obtained with Yb:YAG and Yb:Lu<sub>2</sub>O<sub>3</sub> of 0.66 and 0.72, respectively are in good agreement with previous results at such low output coupling transmissions [36, 41]. The measured laser performance at various low output coupler transmissions below  $4 \times 10^{-3}$  allows to precisely determine an upper limit of the internal resonator losses of a few  $10^{-4}$ , which is about an order of magnitude lower than previously assumed [41, 42]. This also demonstrates the low losses of the thin-disk laser resonator and the excellent quality of the utilized disks, which benefited from improvements in the crystal growth and in optical coating methods over the last decade.

The results in Fig. 3 (b) reveal that intracavity power levels in excess of 0.5 MW can be achieved at pump powers of a few 100 W, even at total resonator losses in the order of  $10^{-3}$ , which would be five times higher than the intracavity losses of  $2 \times 10^{-4}$  we determined for multi-mode linear TDLs using state-of-the-art processed gain materials and standard resonator mirrors. At such intracavity power levels, the required focal intensities for molecular alignment in the order of  $10^{10}$ – $10^{11}$  W/cm<sup>2</sup> could be achieved at realistic intracavity focal diameters of 20–40  $\mu\text{m}$ . Such diameters can be obtained between two concave cavity mirrors and do not impose a particular challenge for the resonator design. Slightly larger intracavity foci have already been demonstrated e.g. in enhancement cavities and conventional resonators [43, 44].

Figure 3 (b) also shows that minimized resonator losses are of crucial importance for achieving high intracavity power levels at moderate pump power levels. We note that we operated our TDL at output coupler transmissions in the order of  $10^{-4}$ . However, in the upcoming experiments the resonator losses will be increased by additional resonator elements, for instance a Brewster plate. At intracavity powers in excess of 100 kW even a very low transmission of  $10^{-7}$  results in leakage of more than 10 mW, which allows for a reliable determination of the intracavity power. Moreover, we expect the main additional losses to occur due to depolarization at polarization control elements, i. e., reflections at Brewster elements or transmission losses at mirrors with a polarization dependent reflectivity. Both should increase resonator extraction efficiency and thus avoid hot-spots in the cavity. Therefore, the disk temperatures should remain lower than demonstrated here, even when using HR mirrors.

The considerations so far were independent of the pump spot diameter on the disk. We have shown that further scaling of the intracavity power may lead to strong heating of the disk. This can be circumvented by choosing larger pump spot diameters, which allows to use

significantly higher pump powers. Even though the alignment sensitivity increases strongly with the laser mode diameter on the disks [45], TDL with centimeter-scale pump spot diameters are reported [46]. Even in fundamental mode operation, a 4.7 mm pump spot diameter has been reported at a pump power of up to 830 W [47]; this corresponds to pump power intensities on the order of 5 kW/cm<sup>2</sup>. In this case the output coupler transmission was optimized for high extraction efficiency, but at the maximum output power of 430 W the remaining pump power deposited in the disk was still as high as 400 W. This pump power level should be sufficient for our experiments.

The application of the laser for molecular alignment requires operation in vacuum and polarization control. Preliminary results in vacuum ( $p = 5 \times 10^{-4}$  mbar) point towards an increased operation stability due to the lack of atmospheric turbulence, in agreement with previous reports [48,49]. Further experiments are required to explore further challenges, e. g., the corresponding lack of convection cooling of the optical elements and mounts. For the alignment experiments it would be sufficient to keep only the focal area of the resonator in a vacuum chamber, but the required additional Brewster windows and polarization optics would add complexity and increase the total resonator losses.

When operated in ultra-high-vacuum ( $10^{-9}$  mbar) and combined with a continuous cold supersonic molecular beam [50], the demonstrated laser system will allow to strongly align and orient molecules at “arbitrary” repetition rates. The continuous presence of aligned molecules will enable the envisioned application of strongly controlled molecules in modern imaging experiments at high-repetition rate X-ray facilities [6, 51].

## 6. Conclusions

We have demonstrated a thin-disk laser providing 135 kW of CW intracavity laser power. This corresponded to an enhancement by a factor of 2500 with respect to the incident pump power of 54 W, enabled by the low losses of state-of-the-art-processed gain disks. The internal round-trip losses of Yb:YAG and Yb:Lu<sub>2</sub>O<sub>3</sub> disks were determined to be about  $2 \times 10^{-4}$ . Calculations show that our approach is scalable and will allow for megawatt-level CW intracavity powers, thus, enabling field-strengths in excess of  $10^{10}$  W/cm<sup>2</sup> in a few-10- $\mu$ m-diameter focus. Such an electric field strengths allow for adiabatic laser alignment or mixed-field orientation of molecules. While pulsed lasers at comparably low repetition rates have been used for this purpose [2, 12, 13, 20], our approach allows for adiabatic alignment at arbitrary repetition rates.

Coupled to a continuous molecular beam, such a setup could allow for the implementation of reactive, chemical scattering investigations of aligned or oriented molecules [52], albeit limited to the very small focal volume ( $10^{-9}$  cm<sup>3</sup>). Moreover, we point out that our laser would also allow for the trapping of atoms and molecules using the polarizability interaction [11, 53]. It would allow for few-Kelvin deep traps for typical small molecules [15] and even deeper traps for larger, more polarizable molecules. This could also be utilized for *in-vacuo* trapping and guiding of nanoparticles [54, 55]. The setup could be useful for many more strong-field experiments in atomic and molecular physics, for instance, at high-repetition-rate FELs [56].

## Acknowledgments

This work has been supported by the excellence cluster “The Hamburg Center for Ultrafast Imaging – Structure, Dynamics and Control of Matter at the Atomic Scale” (CUI) of the Deutsche Forschungsgemeinschaft (DFG EXC1074).